

Characterization of the transcriptome, nucleotide sequence polymorphism, and natural selection in the desert adapted mouse *Peromyscus eremicus*

Matthew D. MacManes¹, Michael B. Eisen²,

¹ Department of Molecular, Cellular and Biomedical Sciences, University of New Hampshire, Durham NH, USA

² HHMI and University of California, Berkeley, Berkeley, CA, USA

* E-mail: macmanes@gmail.com, @PeroMHC

1 Abstract

2 Introduction

3 Deserts are widely considered one of Earth’s most harsh environments. Animals living in desert
 4 environments are forced to endure intense heat and drought, and as a result, species having
 5 evolved in these environments are likely to possess specialized mechanisms that may enhance
 6 fitness. While living in deserts likely involves a large number of adaptive traits, the ability to os-
 7 moregulate – to maintain the proper water and electrolyte balance – appears to be paramount [1].
 8 Indeed, the maintenance of water balance in animals is one of the most important physiologic pro-
 9 cesses for all organisms, whether they be desert inhabitants or not. Most animals are exquisitely
 10 sensitive to changes in osmolality, with slight derangement eliciting physiologic compromise.
 11 When the loss of water exceeds dietary intake, dehydration - and in extreme cases, death - can
 12 occur. This process suggests that there is strong selection for mechanisms supporting osmoreg-
 13 ulation. Understanding these mechanisms will significantly enhance our understanding of the
 14 physiologic processes underlying osmoregulation in extreme environments, having implications
 15 for studies of human health, conservation, and climate change.

16
 17 The genes and structures responsible for the maintenance of water and electrolyte balance
 18 are well characterized in model organisms such as mice [2], rats [3–5], and humans [6–8]. These
 19 studies, many of which have been enabled by newer sequencing technologies, serve as a founda-
 20 tion for studies of renal genomics in non-model organisms. In particular, because researchers
 21 have long been interested in desert adaptation, a number of studies have looked at the mor-
 22 phology or expression of single genes in the renal tissues of desert adapted rodents *Phyllotis*
 23 *darwini* [9], *Psammomys obesus* [10], and *Perognathus penicillatus* [11]. More recently, full re-
 24 nal transcriptomes have been generated for *Dipodomys spectabilis* and *Chaetodipus baileyi* [12]
 25 as well as *Abrothrix olivacea* [13].

These studies provide a rich context for the current and future work, aimed at developing a synthetic understanding of the the genetic and genomic underpinnings of desert adaptation in rodents. As a first step, we have sequenced, assembled, and characterized the transcriptome (using four tissue types - liver, kidney, testes, brain), of a desert adapted cricetid rodent endemic to the Southwest United States [14], *Peromyscus eremicus*. These animals have a lifespan typical of small mammals, and therefore an individual may live it's entire life without ever drinking water. These rodents have distinct advantage over other desert animals (e.g. *Dipodomys*) in that they breed readily in captivity, which enables future laboratory studies of the phenotype of interest. In addition the focal species is positioned in a clade of well known animals (e.g. *P. californicus*, *P. maniculatus* and *P. polionotus*) [15] with growing genetic and genomic resources [16–18] which together suggest that future comparative studies are possible.

While the elucidation of the mechanisms underlying adaptation to desert survival is beyond the scope of this manuscript, we aim here to lay the groundwork by characterizing the transcriptome from four distinct tissues (brain, liver, kidney, testes). These data will be included in current larger effort aimed at sequencing the entire genome. Further, via sequencing the renal tissue of a total of 15 additional animals, we characterize nucleotide polymorphism and genome wide patterns of natural selection. Together, these investigations will aid in our overarching goal – to understand the genetic bases of adaptation to deserts in *P. eremicus*.

Materials and Methods

Animal Collection and Study Design

To begin to understand how genes may underlie desert adaptation, I collected 16 individuals from a single population *P. eremicus* over a two year time period (2012-2013). These individuals were captured in live traps, then euthanized using isoflurane overdose and decapitation. Immediately post-mortem, the abdominal and pelvic organs were removed, cut in half (in the case of kidney), placed in RNAlater and flash frozen in liquid Nitrogen. Removal of the brain, with similar preservation techniques, followed that. Time from euthanasia to removal of all organs never exceeded five minutes. Samples were transferred to a -80C freezer at a later date. These procedures were approved by the University of California Berkeley Animal Care and Use Committee and follow guidelines established by the American Society of Mammalogy for the use of wild animals in research [19].

RNA extraction and Sequencing

Total RNA was extracted from each tissue using a TRIzol extraction (Invitrogen) following the manufacturers instructions. Because preparation of an RNA library suitable for sequencing is dependent on having high quality, intact RNA, a small aliquot of each total RNA extract was analyzed on a Bioanalyzer 2100 (Agilent, Palo Alto, CA, USA). Following confirmation of sample quality, the reference sequencing libraries were made using the TruSeq stranded RNA prep kit (Illumina), while an unstranded TruSeq kit was used to construct the other sequencing libraries. A unique index was ligated to each sample to allow for multiplexed sequencing. Reference libraries (n=4 tissue types) were then pooled to contain equimolar quantities of each individual library and submitted for Illumina sequencing using two lanes of 150nt paired end sequencing using the rapid-mode of the HiSeq 2500 sequencer at The Hubbard Center for Genome Sciences (University of New Hampshire). The remaining 15 libraries were similarly multiplexed and sequenced in a mixture of 100nt paired and single end across two lanes of an Illumina HiSeq 2000 at the Vincent G. Coates Gnome Center (University of California, Berkeley).

Sequence Data Preprocessing and Assembly

The raw sequence reads were error corrected using the software *bleed* [20], using *kmer*=25, based on the developers default recommendations. The error corrected adapter and quality trimmed following recommendations from MacManes [21] and Mbandi [22]. Specifically, adapter sequence contamination was removed, and low quality nucleotides (defined as PHRED <2) were removed using the program Trimmomatic version 0.32 [23]. Reads from each tissue were assembled using Trinity version released 17 July 2014 [24]. We used flags indicating the stranded nature of sequencing reads and set maximum allowable physical distance between read pairs to 999nt. The assembly was conducted on a linux workstation with 64 cores and 512Gb RAM. To filter the raw sequence assembly, I downloaded *Mus musculus* cDNA and ncRNA datasets from Ensembl (ftp://ftp.ensembl.org/pub/release-75/fasta/mus_musculus/), and the *Peromyscus maniculatus* reference transcriptome from NCBI (ftp://ftp.ncbi.nlm.nih.gov/genomes/Peromyscus_maniculatus_bairdii/RNA/). I used a blastN procedure (default settings, *evalue* set to 10^{-10}) to identify contigs in the *P. eremicus* dataset that are likely biological in origin. This procedure, when a reference dataset is available, retains more putative transcripts than a strategy employing expression-based filtering (remove if *TMP* <1) of the raw assembly. I then concatenated the filtered assemblies from each tissue into a single file, reducing redundancy using the software *cd-hit-est* [25] using default setting except that sequences were clustered based on 95% sequence similarity.

91 Assembled Sequence Annotation

92 The filtered assemblies were annotated using default settings of the blastN algorithm [26]
 93 against the Ensembl cDNA and ncRNA datasets described above, downloaded on 1 August
 94 2014. Amongst other things, the Ensemble transcript identifiers were used in the analysis
 95 of gene ontology, conducted in the PANTHER package [27]. Next, because rapidly evolv-
 96 ing nucleotide sequences may evade detection by blast algorithms, we used HMMER3 [28] to
 97 search for conserved protein domains contained in the dataset using the Pfam database [29].
 98 Lastly, I extracted putative coding sequences using Transdecoder version 4Jul2014 (<http://transdecoder.sourceforge.net/>)
 99

100
 101 To identify patterns of gene expression unique to each tissue type, I mapped sequence reads
 102 from each tissue type to the reference assembly using bwa-mem [30]. We estimated expression
 103 individually for the four tissues using default settings of the software eXpress [31]. Interesting
 104 patterns of expression, including instances where expression was limited to a single tissue type
 105 were identified and visualized.
 106

107 Population Genomics

108 In addition to the reference individual sequenced at four different tissue types, we sequenced
 109 15 other conspecific individuals from the same population, located in Palm Desert, California.
 110 Sequence data were mapped to the reference transcriptome using bwa-mem. The alignments
 111 were sorted and converted to BAM format, then passed to the program ANGSD version 0.610,
 112 which was used for calculating the folded site frequency spectrum (SFS) and Tajima's D [32].
 113

114 Natural Selection

115 To characterize natural selection on several genes related to water and ion homeostasis, we
 116 identified several of the transcripts identified as experiencing positive selection in a recent work
 117 on desert-adapted *Dipodomys* rodents. The coding sequence corresponding to these genes, Solute
 118 Carrier family 2 member 9 (Slc2a9) and the Vitamin D3 receptor (Vdr), were extracted from
 119 the dataset, aligned using the software MACSE [33] to homologous sequences in *Mus musculus*,
 120 *Rattus norvegicus*, *Peromyscus maniculatus*, and *Homo sapiens* identified by the conditional
 121 reciprocal best blast procedure (CRBB, [34]). An unrooted gene tree was constructed using the
 122 online resource Clustal-Omega, and together the tree and alignment were analyzed using the
 123 branch-site model (model=2, nsSites=2, fix_omega=0 versus model=2, nsSites=2, fix_omega=1,

124 omega=1) implemented in PAML version 4.8 [35,36].

125 Results

126 RNA extraction, Sequencing, Assembly, Mapping

127 RNA was extracted from the hypothalamus, renal medulla, testes, or liver from each individual
 128 using sterile technique. TRIzol extraction resulted in a large amount of high quality ($RIN \geq 8$)
 129 total RNA, which was used as input. Libraries were constructed as per the standard Illumina
 130 protocol, and were sequenced as described above. The number of reads per library varied from
 131 56 million strand-specific paired-end reads in Peer360 kidney, to 9 million single-end reads in
 132 Peer321. Adapter sequence contamination and low-quality nucleotides were eliminated, which
 133 resulted in a loss of <2% of reads.

134
 135 Transcriptome assembly for each tissue type was accomplished using the program Trin-
 136 ity [24]. The raw assembly for brain, liver, testes and kidney contained 185425, 222096, 180233,
 137 and 514091 assembled sequences respectively. This assembly was filtered using a blastN pro-
 138 cedure against the *Mus* cDNA and ncRNA which resulted in a final dataset containing 68331
 139 brain-specific transcripts, 71041 liver-specific transcripts, 67340 testes-specific transcripts, and
 140 113050 kidney-specific transcripts. Mapping the error-corrected adapter/quality trimmed reads
 141 to these datasets resulted in mapping 94.98% (87.01% properly paired) of brain-derived reads
 142 to the brain transcriptome, 96.07% (88.13% properly paired) of liver-derived reads to the liver
 143 transcriptome, 96.81% (85.10% properly paired) of testes-derived reads to the testes transcrip-
 144 tome, and 91.87% (83.77% properly paired) of kidney-derived reads to the kidney transcriptome.
 145 Together, these statistics suggest that the tissue-specific transcriptomes are of extremely high
 146 quality.

147

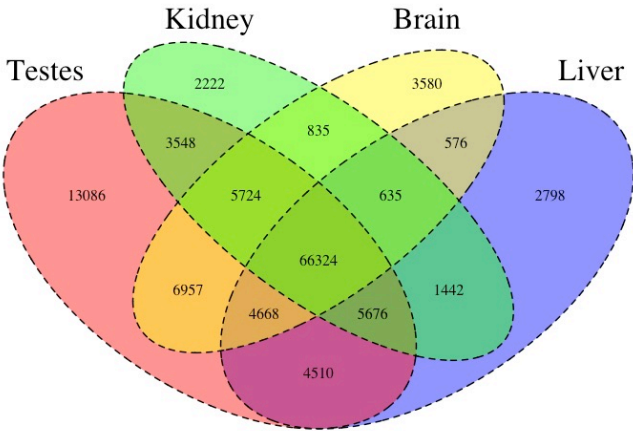


Figure 1. The Venn Diagram.

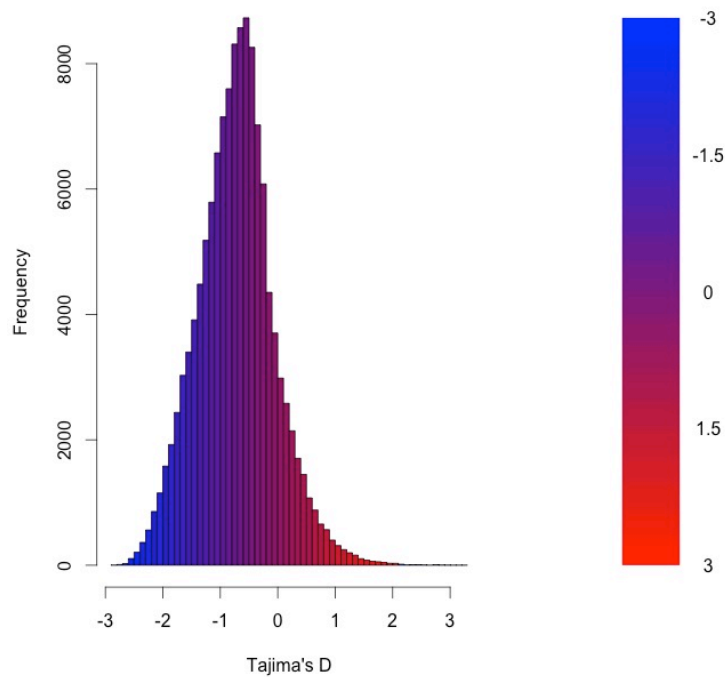
I then estimated gene expression on each of these tissue-specific datasets, which allowed me to understand expression patterns in the multiple tissues (Figure 1). After expression estimation, the filtered assemblies were concatenated together, and after removal of redundancy with cd-hit-est, 123,123 putative transcripts remained. From this filtered concatenated dataset, I extracted 71626 putative coding sequences (72Mb). Of these 71626 sequences, 38221 were complete exons (containing both start and stop codons), while other were either truncated at the 5-prime end (20239 sequences), 3-prime end (6445 sequences), or were internal (6721 sequencing having neither stop nor start codon).

Transcript ID	Testes	Liver	Kidney	Brain	Genbank ID	Gene ID
Transcript_83842	2.05E+03	6.40E+03	1.03E+04	5.47E+03	DQ073446.1	COX2
Transcript_126459	1.43E+01	2.22E+04	2.77E+01	6.73E+00	XM_006991665.1	Alb
Transcript_128937	4.39E+00	1.91E+04	4.74E+02	2.23E+00	XM_007627625.1	Apoa2
Transcript_81233	1.71E+03	5.23E+03	6.11E+03	3.08E+03	XM_006993867.1	Fth1
Transcript_94125	3.67E+01	1.08E+04	2.09E+03	2.75E+00	XM_006977178.1	CytP450
Transcript_119945	5.03E+03	1.15E+03	1.33E+03	3.71E+03	XM_008686011.1	Ubb
Transcript_5977	4.95E+00	1.01E+04	3.05E+02	3.58E+02	XM_006978668.1	Tf
Transcript_4057	2.62E+01	9.32E+03	1.34E+02	8.38E+01	XM_006994871.1	Apoc1
Transcript_112523	4.07E+02	7.36E+03	7.78E+02	9.54E+02	XM_006994872.1	Apoe
Transcript_98376	1.98E+00	8.66E+03	1.02E+00	2.68E+00	XM_006970208.1	Ttr

Table 2. The 10 transcripts with the highest mean TPM (transcripts per million).

160 Population Genomics

161 As detailed above, the RNAseq data from 15 individuals were mapped to the reference tran-
 162 scriptome with the resulting BAM files being used as input to the software package ANGSD.
 163 The Tajima's D statistic was calculated for all transcripts covered by at least 14 of the 15 indi-
 164 viduals. The distribution of the results, shown in Figure 2, suggest that the vast majority of the
 165 transcriptome is under purifying selection ($D < 0$), with a much smaller fraction being subject
 166 to neutral or positive selection.



167 Figure 2. Tajima's D

Transcript ID	GenBank ID	Description	Tajima's D
Transcript_49049	XM_006533884.1	heterogeneous nuclear ribonucleoprotein H1 (Hnrnp1)	3.26
Transcript_38378	XM_006522973.1	Son DNA binding protein (Son)	3.19
Transcript_126187	NM_133739.2	transmembrane protein 123 (Tmem123)	3.02
Transcript_70953	XM_006539066.1	chloride channel Kb (Clcnkb)	2.96
Transcript_37736	XM_006997718.1	h-2 class I histocompatibility antigen	2.92
Transcript_21448	XM_006986148.1	zinc finger protein 624-like	2.84
Transcript_47450	NM_009560.2	zinc finger protein 60 (Zfp60)	2.82
Transcript_122250	XM_006539068.1	chloride channel Kb (Clcnkb)	2.81
Transcript_78367	XM_006496814.1	CDC42 binding protein kinase alpha (Cdc42bpa)	2.78
Transcript_96470	XM_006987129.1	interferon-inducible GTPase 1-like	2.77

Table 4. The 10 transcripts with the highest values for Tajima's D, which is suggestive of positive selection.

Transcript ID	GenBank ID	Description	Tajima's D
Transcript_84359	XM_006991127.1	nuclear receptor coactivator 3 (Ncoa3)	-2.82
Transcript_87121	XM_006970128.1	methyl-CpG binding domain protein 2 (Mbd2)	-2.82
Transcript_125755	EU053203.1	alpha globin gene cluster	-2.78
Transcript_87128	XM_006976644.1	membrane-associated ring finger (March5)	-2.76
Transcript_55468	XM_006978377.1	Vpr (HIV-1) binding protein (Vprbp)	-2.75
Transcript_116042	XM_006980811.1	membrane associated guanylate kinase (Magi3)	-2.75
Transcript_18966	XM_006982814.1	ubiquitin protein ligase E3 component n-recognin 5 (Ubr5)	-2.75
Transcript_122204	XM_008772511.1	zinc finger protein 612 (Zfp612)	-2.75
Transcript_100550	XM_006971297.1	bromodomain adjacent to zinc finger domain, 1B (Baz1b)	-2.74
Transcript_33267	XM_006975561.1	pumilio RNA-binding family member 1 (Pum1)	-2.75

Table 3. The 10 transcripts with the lowest values for Tajima's D, which is suggestive of purifying selection.

172 Natural Selection

173 To test the hypothesis that selection on transcripts related to osmoregulation is enhanced in the
174 desert adapted *P. eremicus*, I implemented the branch-site test as described above, setting the
175 sequence corresponding to *P. eremicus* for both Slc2a9 and Vdr as the foreground lineages in
176 2 distinct program executions. The test for Slc2a9 was highly significant ($2\Delta\text{Lnl}=51.4$, $\text{df}=1$,
177 $p=0$), indicating enhanced selection in *P. eremicus* relative to the other lineages. The branch
178 site test for positive selection conducted on the Vdr gene was non-significant ($2\Delta\text{Lnl}=0.68$, $\text{df}=1$,
179 $p=1$).

Discussion

Acknowledgments

References

1. Walsberg G (2000) Small mammals in hot deserts: Some generalizations revisited. *Bio-science* 50: 109–120.
2. Tatum R, Zhang Y, Salleng K, Lu Z, Lin JJ, et al. (2009) Renal salt wasting and chronic dehydration in claudin-7-deficient mice. *AJP: Renal Physiology* 298: F24–F34.
3. Romero DG, Plonczynski MW, Welsh BL, Gomez-Sanchez CE, Zhou MY, et al. (2007) Gene expression profile in rat adrenal zona glomerulosa cells stimulated with aldosterone secretagogues. *Physiological Genomics* 32: 117–127.
4. Rojek A, Rojek A, Fuchtbauer E, Fuchtbauer E, Kwon T, et al. (2006) Severe urinary concentrating defect in renal collecting duct-selective AQP2 conditional-knockout mice. *Proceedings of The National Academy of Sciences of The United States of America* 103: 6037–6042.
5. Nielsen S, Chou C, Marples D, Christensen E, Kishore B, et al. (1995) Vasopressin Increases Water Permeability of Kidney Collecting Duct by Inducing Translocation of Aquaporin-Cd Water Channels to Plasma-Membrane. *Proceedings of The National Academy of Sciences of The United States of America* 92: 1013–1017.
6. Mobasheri A, Marples D, Young IS, Floyd RV, Moskaluk CA, et al. (2007) Distribution of the AQP4 Water Channel in Normal Human Tissues: Protein and Tissue Microarrays Reveal Expression in Several New Anatomical Locations, including the Prostate Gland Seminal Vesicles. *Channels* 1: 30–39.
7. Bedford JJ, Leader JP, Walker RJ (2003) Aquaporin expression in normal human kidney and in renal disease. *Journal of the American Society of Nephrology : JASN* 14: 2581–2587.
8. Nielsen S, Kwon T (1999) Physiology and Pathophysiology of Renal Aquaporins. *Journal of the ...*
9. Gallardo PA, Cortés A, Bozinovic F (2005) Phenotypic flexibility at the molecular and organismal level allows desert-dwelling rodents to cope with seasonal water availability. *Physiological and Biochemical Zoology* 78: 145–152.

- 210 10. Kaissling B, De Rouffignac C, Barrett JM, Kriz W (1975) The structural organization
211 of the kidney of the desert rodent *Psammomys obesus*. *Anatomy and embryology* 148:
212 121–143.
- 213 11. Altschuler EM, Nagle RB, Braun EJ, Lindstedt SL, Kruttsch PH (1979) Morphological
214 study of the desert heteromyid kidney with emphasis on the genus *Perognathus*. *The*
215 *Anatomical record* 194: 461–468.
- 216 12. Marra NJ, Romero a, DeWoody Ja (2014) Natural selection and the genetic basis of
217 osmoregulation in heteromyid rodents as revealed by RNA-seq. *Molecular Ecology* 23:
218 2699–2711.
- 219 13. Giorello FM, Feijoo M, a GD, Valdez L, Opazo JC, et al. (2014) Characterization of the
220 kidney transcriptome of the South American olive mouse *Abrothrix olivacea* 15: 1–10.
- 221 14. Veal R, Caire W (2001) *Peromyscus eremicus*. *Mammalian Species* 118: 1–6.
- 222 15. Feng BJ, Sun LD, Soltani-Arabshahi R, Bowcock AM, Nair RP, et al. (2007) Toward
223 a Molecular Phylogeny for *Peromyscus*: Evidence from Mitochondrial Cytochrome- b
224 Sequences. *Journal of Mammalogy* 88: 1146–1159.
- 225 16. Shorter KR, Owen A, anderson V, Hall-South AC, Hayford S, et al. (2014) Natural Ge-
226 netic Variation Underlying Differences in *Peromyscus* Repetitive and Social/Aggressive
227 Behaviors. *Behavior genetics* .
- 228 17. Panhuis TM, Broitman-Maduro G, Uhrig J, Maduro M, Reznick DN (2011) Analysis of
229 Expressed Sequence Tags from the Placenta of the Live-Bearing Fish *Poeciliopsis* (Poe-
230 ciliidae). *Journal of Heredity* 102: 352–361.
- 231 18. Shorter KR, Crossland JP, Webb D, Szalai G, Felder MR, et al. (2012) *Peromyscus* as a
232 Mammalian Epigenetic Model. *Genetics Research International* 2012: 1–11.
- 233 19. Sikes RS, Gannon WL, Animal Care and Use Committee of the American Society of
234 Mammalogists (2011) Guidelines of the American Society of Mammalogists for the use of
235 wild mammals in research. *Journal of Mammalogy* 92: 235–253.
- 236 20. Heo Y, Wu XL, Chen D, Ma J, Hwu WM (2014) BLESS: bloom filter-based error cor-
237 rection solution for high-throughput sequencing reads. *Bioinformatics* (Oxford, England)
238 30: 1354–1362.
- 239 21. MacManes MD (2014) On the optimal trimming of high-throughput mRNA sequence
240 data. *Frontiers in Genetics* 5.

- 241 22. Christoffels A (2014) A glance at quality score: implication for *de novo* transcriptome
242 reconstruction of Illumina reads : 1–5.
- 243 23. Lohse M, Bolger AM, Nagel A, Fernie AR, Lunn JE, et al. (2012) RobiNA: a user-friendly,
244 integrated software solution for RNA-Seq-based transcriptomics. *Nucleic Acids Research*
245 40: W622–7.
- 246 24. Haas BJ, Papanicolaou A, Yassour M, Grabherr M, Blood PD, et al. (2013) *De novo*
247 transcript sequence reconstruction from RNA-seq using the Trinity platform for reference
248 generation and analysis. *Nature protocols* 8: 1494–1512.
- 249 25. Li W, Godzik A (2006) Cd-hit: a fast program for clustering and comparing large sets of
250 protein or nucleotide sequences. *Bioinformatics (Oxford, England)* 22: 1658–1659.
- 251 26. Camacho C, Coulouris G, Avagyan V, Ma N, Papadopoulos J, et al. (2009) BLAST+:
252 architecture and applications. *BMC Bioinformatics* 10: 421.
- 253 27. Mi H (2004) The PANTHER database of protein families, subfamilies, functions and
254 pathways. *Nucleic Acids Research* 33: D284–D288.
- 255 28. Wheeler TJ, Eddy SR (2013) nhmmer: DNA homology search with profile HMMs. *Bioin-*
256 *formatics (Oxford, England)* 29: 2487–2489.
- 257 29. Punta M, Coggill PC, Eberhardt RY, Mistry J, Tate J, et al. (2012) The Pfam protein
258 families database. *Nucleic Acids Research* 40: D290–301.
- 259 30. Li H (2013) Aligning sequence reads, clone sequences and assembly contigs with BWA-
260 MEM .
- 261 31. Roberts A, Pachter L (2013) Streaming fragment assignment for real-time analysis of
262 sequencing experiments. *Nature Methods* 10: 71–73.
- 263 32. Korneliussen TS, Moltke I, Albrechtsen A (2013) Calculation of Tajima’s D and other
264 neutrality test statistics from low depth next-generation sequencing data. *BMC*
- 265 33. Ranwez V, Harispe S, Delsuc F, Douzery EJP (2011) MACSE: Multiple Alignment of
266 Coding SEquences Accounting for Frameshifts and Stop Codons. *PLOS ONE* 6: e22594.
- 267 34. Aubry S, Kelly S, Kämpers BMC, Smith-Unna RD, Hibberd JM (2014) Deep Evolutionary
268 Comparison of Gene Expression Identifies Parallel Recruitment of Trans-Factors in Two
269 Independent Origins of C4 Photosynthesis. *PLOS Genetics* 10: e1004365.

270 35. Yang Z, dos Reis M (2011) Statistical Properties of the Branch-Site Test of Positive
271 Selection. Molecular Biology and Evolution 28: 1217–1228.

272 36. Yang Z (2007) PAML 4: Phylogenetic Analysis by Maximum Likelihood. Molecular
273 Biology and Evolution 24: 1586–1591.

274 **Figure Legends**

275 **Tables**

276 **Table 1**

277

DATASET	NUM. RAW READS
PEER360 TESTES	32M PE
PEER360 LIVER	53M PE
PEER360 KIDNEY	56M PE
PEER360 BRAIN	23M PE
PEER305	19M PE
PEER308	15M PE
PEER319	14M PE
PEER321	9M SE
PEER340	16M PE
PEER352	14M PE
PEER354	9M SE
PEER359	14M PE
PEER365	16M PE
PEER366	16M PE
PEER368	14M PE
PEER369	14M PE
PEER372	17M SE
PEER373	23M SE
PEER380	16M SE
PEER382	14M SE

278

279 Table 1. The number of sequencing reads per sample